Research Article
Open Access
CrossMark

Dynamic modeling of nitrogen adsorption on zeolite 13x bed

Abstract

Generally, the common adsorption processes of air separation are divided into two categories: The first category is consists of processes which make use of zeolites as nitrogen adsorbent under the equilibrium conditions and oxygen is a process product. The second one contains processes which utilize Carbon Molecular Sieves (CMSs) as oxygen adsorbent. Zeolite 13X is the most commonly adsorbent used in the air separation for oxygen production. In this work, nitrogen adsorption behavior on zeolite 13X bed is simulated. Desorption and adsorption dynamics of zeolite 13X was investigated in order to study the behavior of this zeolite. The simulation results showed that the high Roll-up Phenomena occurs for oxygen than nitrogen. There is a large mass transfer zone (MTZ) for zeolite 13X. Therefore, the adsorption rate of zeolite 13X is high. The main drop of nitrogen concentration in the outlet of zeolite 13X occurs at the time of about 125 seconds. Nitrogen concentration in the outlet of zeolite 13X approaches zero after about 180 seconds.

Keywords: nitrogen adsorption, zeolite 13x, simulation study

Volume 1 Issue 1 - 2017

Iman Ahmadi Kakavandi,[1] Ehsan Javadi Shokroo,[2] Mehdi Baghbani,[3] Mehdi Farniaei[4]

[1]Commercialization Department, FAPKCO Engineering Group, Iran

[2]Research Team, FAPKCO Engineering Group, Iran

[3]Support Team, FAPKCO Engineering Group, Iran

[4]Research Team, FAPKCO Engineering Group, Iran

Correspondence: Ehsan Javadi Shokroo, FAPKCO Engineering Group, Sanaye Sq., Mirzaye Shirazi Blvd., Shiraz, Fars, Iran, Tel +989178688600, Fax +987136362782, Email ehsan.javadi@hotmail.com

Received: June 10, 2017 | **Published:** August 31, 2017

Introduction

Oxygen is one of the most important products in chemical industries. This chemical element is used in various processes such as: refinery industries, manufacturing metal and other industrial operations. For instance, oxygen with high purity is utilized in different chemical processes like: steel construction, paper industries, wastewater treatment and glass production. In 1907, oxygen was produced for the first time, when Linde built a first cryogenic distillation bed for air separation.[1] Zeolite 13X is the most commonly adsorbent used in the air separation for oxygen production. The unique properties of zeolites are originated from this fact that their surfaces are formed with negatively charged oxides. Moreover, the presence of isolated cations above their surface structure is another reason for their uniqueness. Zeolites are aluminosilicate crystallines of alkaline or earth alkaline elements such as sodium, potassium and calcium. nGenerally, the common adsorption processes of air separation are divided into two categories: The first category is consists of processes which make use of zeolites as nitrogen adsorbent under the equilibrium conditions and oxygen is a process product.

The second one contains processes which utilize Carbon Molecular Sieves (CMSs) as oxygen adsorbent. Based on kinetic separation in this kind of category, oxygen is adsorbed owing to its faster permeation and higher selectivity. Moreover, nitrogen is produced as a product in such these processes.

The unique properties of zeolites originate from the fact that their surfaces are formed with negatively charged oxides. Moreover, the presence of isolated cations above their surface structure is another reason for their uniqueness. Despite the known selectivity of N_2/O_2 by zeolites, there had not been progress in the case of air separation by adsorption process until 1960, even after the innovation of synthetic zeolites A and X and cycles of PSA. The innovation of zeolites A and X by Milton[1] in1959 created conditions which were always available. By the enthusiasm of these innovations, the industrial ideologist was encouraged to examine the feasibility of air separation at ambient temperature by applying adsorption processes (in contrast to 77k for cryogenic processes).

Zeolite 13X is the most commonly used adsorbent in the air separation for oxygen production. Zeolites are aluminosilicate crystallines of alkaline or earth alkaline elements such as sodium, potassium and calcium. Detailed description of zeolites structure is accessible in relevant sources.[2,3] There are a lot of studies which have been done on the separation of oxygen from air.[4–19]

Oxygen is one of the most important products in chemical industries. This chemical element is used in various processes such as: refinery industries, manufacturing metal and other industrial operations. For instance, oxygen with high purity is utilized in different chemical processes like: steel construction, paper industries, wastewater treatment and glass production. In 1907, oxygen was produced for the first time, when Linde built a first cryogenic distillation bed for air separation.[1]

In this work, the adsorption of nitrogen using zeolite 13X as adsorbents is simulated. The dynamic of nitrogen adsorption is examined. The simulated PSA process is depicted in Figure 1.

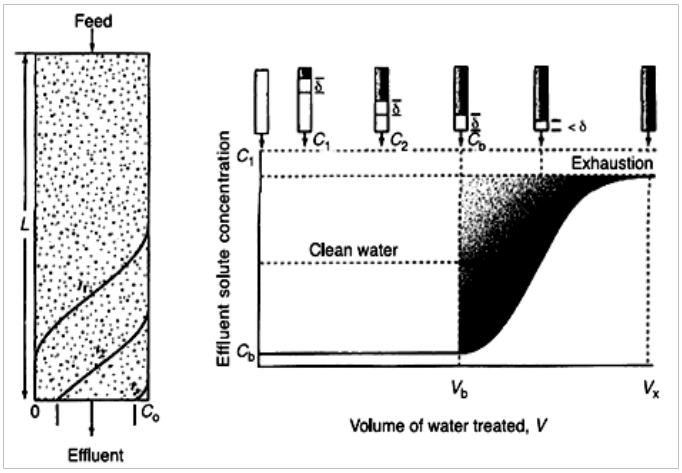

Figure 1 Schematic diagram of the adsorption bed.[3]

Mathematical model

In order to develop a mathematical model for an adsorption bed, the following assumptions were made:

Gas behaves as an ideal gas;

The flow pattern is axially assumed as plug-flow model;

Equilibrium equations for air are expressed as triple Langmuir-Freundlich isotherm (oxygen, nitrogen and argon);

Rate of mass transfer is presented by linear driving force (LDF) relations;

Bed is clean at initial state and there is no gas flow in it;

Air is considered a mixture of oxygen and argon (21%) and nitrogen (79%) as feed.

According to these assumptions, dynamic behavior of system in terms of mass, energy and momentum balances can be expressed as follows:

Dimensionless partial mass balance for gas phase in the adsorption bed is:[2,9–11]

$$-\left(\frac{1}{P_e^m}\right).\frac{\partial^2 y_i}{\partial \bar{z}^2}+y_i.\frac{\partial \hat{u}}{\partial \bar{z}}+\hat{u}.\left(\frac{\partial y_i}{\partial \bar{z}}+y_i.\left(\frac{1}{\hat{P}}.\frac{\partial \hat{P}}{\partial \bar{z}}-\frac{1}{\hat{T}}.\frac{\partial \hat{T}}{\partial \bar{z}}\right)\right)+\frac{\partial y_i}{\partial \tau}+$$
$$y_i.\left(\frac{1}{\hat{P}}.\frac{\partial \hat{P}}{\partial \tau}-\frac{1}{\hat{T}}.\frac{\partial \hat{T}}{\partial \tau}\right)+\left(\frac{\rho_p.R.T_0.\hat{T}}{P_0.\hat{P}}\right).\left(\frac{1-\varepsilon}{\varepsilon}\right).\left(q_{m,i}.\frac{\partial \hat{q}_i}{\partial \tau}+\hat{q}_i.\frac{\partial q_{m,i}}{\partial \tau}\right)=0 \quad (1)$$

Dimensionless equilibrium loading of i^{th} component for solid phase in the adsorption bed is:

$$\frac{\partial q_{m,i}}{\partial \tau}=\frac{\partial q_{m,i}}{\partial \hat{T}}\times\frac{\partial \hat{T}}{\partial \tau}=k_{2,i}T_0\times\frac{\partial \hat{T}}{\partial \tau} \quad (2)$$

Dimensionless loading of ith component for solid phase in the adsorption bed is (LDF relation):

$$\frac{\partial \hat{q}_i}{\partial \tau}=\alpha_i.\left(\frac{\beta_i.y_i^{ni}}{1+\sum_{j=1}^{N}\beta_j.y_j^{nj}}-\hat{q}_i\right)-\left(\frac{\hat{q}_i}{q_{m,i}}.\frac{\partial q_{m,i}}{\partial \tau}\right) \quad (3)$$

According to equation (3), the LDF relation depends on various parameters such as: equilibrium parameter for the Langmuir model, mole fraction of species i in the gas phase, average amount adsorbed and equilibrium parameter for the Langmuir model.

The equilibrium of triple Langmuir-Freundlich isotherm is as follows:

$$\hat{q}_i^*=\frac{\beta_i y_i^{ni}}{1+\sum_{j=1}^{N}\beta_j.y_j^{nj}} \quad (4)$$

Where β, n and q_m are as follows:

$$q_{m,i}=k_1+k_2T_0\hat{T} \quad (5)$$

$$\beta_i=k_3\exp\left(\frac{k_4}{T_0\hat{T}}\right) \quad (6)$$

$$n=k_5+\frac{k_6}{T_0\hat{T}} \quad (7)$$

Adsorption isotherm parameters and diffusion rate constants of oxygen, nitrogen and argon over zeolite 13X is presented in Table 1.

Table 1 Equilibrium parameters and adsorption heat of oxygen, nitrogen and argon on zeolite 13X[12]

Parameters	N_2	O_2
$k_1\times10^3$ (mol/g)	12.52	6.705
$k_2\times10^5$ (mol/g.K)	-1.785	-1.435
$k_3\times10^4$ (1/atm)	2.154	3.253
k_4 (K)	2333	1428
k_5	1.666	-0.3169
k_6 (K)	-245.2	387.8
Heat of adsorption, (cal/mol)	4390	3060
LDF constant (s^{-1})	0.197	0.62

Overall dimensionless mass balance for gas phase in the adsorption bed is:[4,12–14]

$$\left(\frac{1}{\hat{P}}\right).\frac{\partial \hat{P}}{\partial \tau}+\frac{\partial \hat{u}}{\partial \bar{z}}+\frac{\hat{u}}{\hat{P}}.\frac{\partial \hat{P}}{\partial \bar{z}}-\left(\frac{1}{\hat{T}}\right).\left(\frac{\partial \hat{T}}{\partial \tau}+\hat{u}\frac{\partial \hat{T}}{\partial \bar{z}}\right)+\left(\frac{\rho_p.R.T_0.\hat{T}}{P_0.\hat{P}}\right).\left(\frac{1-\varepsilon}{\varepsilon}\right).$$
$$\sum_{i=1}^{3}\left(q_{m,i}.\frac{\partial \hat{q}_i}{\partial \tau}+\hat{q}_i.\frac{\partial q_{m,i}}{\partial \tau}\right)=0 \quad (8)$$

Dimensionless energy balance for gas phase in the adsorption bed is:[5–7,10,16]

$$-\left(\frac{1}{P_e^h}\right).\frac{\partial^2 \hat{T}}{\partial \bar{z}^2}+\varepsilon.\left(\hat{u}\frac{\partial T}{\partial \bar{z}}+\hat{T}\frac{\partial \hat{u}}{\partial \bar{z}}\right)+\left(\varepsilon_t+\frac{\rho_B.c_{p,s}}{\rho_g.c_{p,g}}\right).\frac{\partial \hat{T}}{\partial \tau}-\left(\frac{\rho_B}{T_0.\rho_g.c_{p,g}}\right).$$
$$\sum_{i=1}^{3}\left[\left(q_{m,i}.\frac{\partial \hat{q}_i}{\partial \tau}+\hat{q}_i.\frac{\partial q_{m,i}}{\partial \tau}\right)\left(-\Delta\bar{H}_i\right)\right]+\left(\frac{2h_i.L}{R_{B,i}.U_0.\rho_g.c_{p,g}}\right).\left(\hat{T}-\hat{T}_w\right)=0 \quad (9)$$

Dimensionless energy balance for the wall of adsorption bed is:

$$\frac{\partial \hat{T}_w}{\partial \tau}=\left[\frac{2\pi.R_{B,i}.h_i.L}{\rho_w.c_{p,w}.A_w.U_0}\right].\left(\hat{T}-\hat{T}_w\right)-\left[\frac{2\pi.R_{B,o}.h_o.L}{\rho_w.c_{p,w}.A_w.U_0}\right].\left(\hat{T}_w-\frac{T_{atm}}{T_0}\right) \quad (10)$$

Cross-sectional area of adsorption bed wall is:

$$A_w=\pi.\left(R_{B,o}^2-R_{B,i}^2\right) \quad (11)$$

Ergun equation is utilized in order to investigate the pressure drop across the adsorption bed.[8,9]

$$-\frac{d\hat{P}}{d\bar{z}}=\left[a.\mu.U_0.\hat{u}+b.\rho.U_0^2.\hat{u}.|\hat{u}|\right].\left(\frac{L}{P_0}\right) \quad (12)$$

Citation: Kakavandi IA, Shokroo EJ, Baghbani M, et al. Dynamic modeling of nitrogen adsorption on zeolite 13x bed. *Fluid Mech Res Int.* 2017;1(1):20–24. DOI: 10.15406/fmrij.2017.01.00004

$$a=\frac{150}{4R_p^2}\cdot\frac{(1-\varepsilon)^2}{\varepsilon^2};b=1.75\frac{(1-\varepsilon)}{2R_p\varepsilon} \quad (13)$$

Physical properties of adsorbents and characteristics of adsorption bed are depicted in (Tables 2 & 3), respectively.

Table 2 Physical properties of bed and adsorbent[12]

Characteristic	Zeolite 13X
Type	Sphere
Average pellet size, R_p (cm)	0.07
Pellet density, ρ_p (g/cm^3)	1.17
Heat capacity, C_{ps} (cal/g.K)	0.32
Bed porosity, ε	0.391
Bed density, ρ_B (g/cm^3)	0.713

Table 3 Adsorption bed properties[21]

Characteristic	Zeolite 13X
Length, L (cm)	76
Inside radius, R_{Bi} (cm)	2.138
Outside radius, R_{Bo} (cm)	2.415
Heat capacity of the column, C_{pw} (cal/g.K)	0.12
Density of column, ρ_W (g/cm^3)	7.83
Internal heat-transfer coefficient, h_i (cal/cm^2.K.s)	9.2×10^{-4}
External heat-transfer coefficient, h_o (cal/ cm^2.K.s)	3.4×10^{-4}
Axial thermal conductivity, K_L (cal/cm.s.K)	6.2×10^{-5}
Axial dispersion coefficient, D_L (cm^2/s)	1×10^{-5}

Results and discussion

The fourth order Runge-Kutta Gill scheme was used to solve a mathematical model considered as coupled partial differential equations. The experimental data obtained from literatures has been simulated in order to validate the simulation results in this study.[9,12,13] An experimental and simulation study of a PSA unit which is running a traditional Skarstrom cycle and a Skarstrom cycle with co-current equalization owing to separate oxygen from air using a 5A zeolite has been proposed by Mendes et al.[9] Moreover, a small-scale two-bed six-step PSA process using zeolite 13X was performed by Jee et al.,[20] in order to provide oxygen-enriched air. They showed that there is a strong effect of feed flow rate on O_2 purity.[12] The effects of adsorption and desorption on zeolite 5A and CMS beds were investigated in a mixture of N2/O2/Ar by Jee et al.[13] A non-isothermal mathematical model was applied in order to simulate the adsorption dynamics in their studies.

Figures 2 (A) & (B) indicate the effect of product flow rate and P/F on the purity and recovery of oxygen during PSA process, respectively. The impact of temperature variations in gas phase during adsorption as a function of time is illustrated in Figure 2 (C). It is obviously seen that there is a relatively high accuracy in the simulation of experimental data.[21]

Breakthrough curves for nitrogen and oxygen on zeolite 13X is shown in Figure 3. The term "break-through time" is originated from the response of initially cleaned bed per a flow with a constant composition. As an initial condition, it is assumed that the adsorption bed is pressurized with a non-adsorptive gas. As shown in Figure 3, oxygen exits from the top of zeolite 13X earlier than nitrogen at a time of approximately 230seconds.[21]

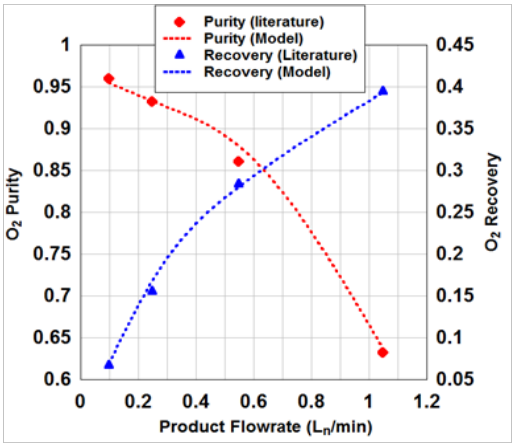

Figure 2 (A) Numerical simulation of experimental data in this work.[9]

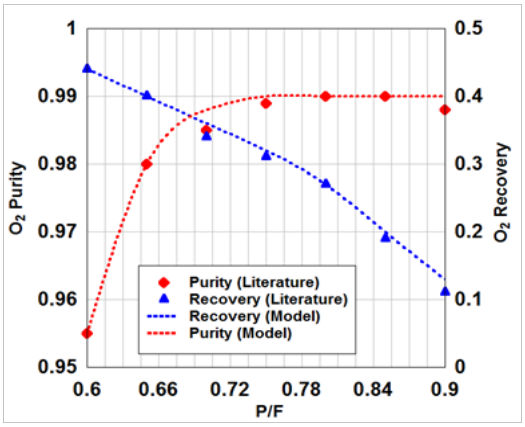

Figure 2 (B) Numerical simulation of experimental data in this work.[12]

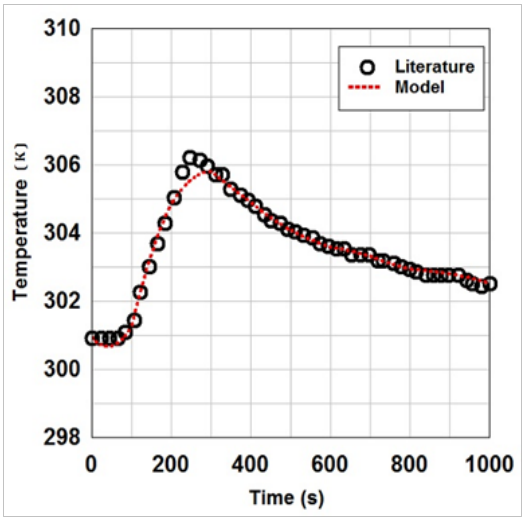

Figure 2 (C) Numerical simulation of experimental data in this work.[13]

Citation: Kakavandi IA, Shokroo EJ, Baghbani M, et al. Dynamic modeling of nitrogen adsorption on zeolite 13x bed. *Fluid Mech Res Int.* 2017;1(1):20–24. DOI: 10.15406/fmrij.2017.01.00004

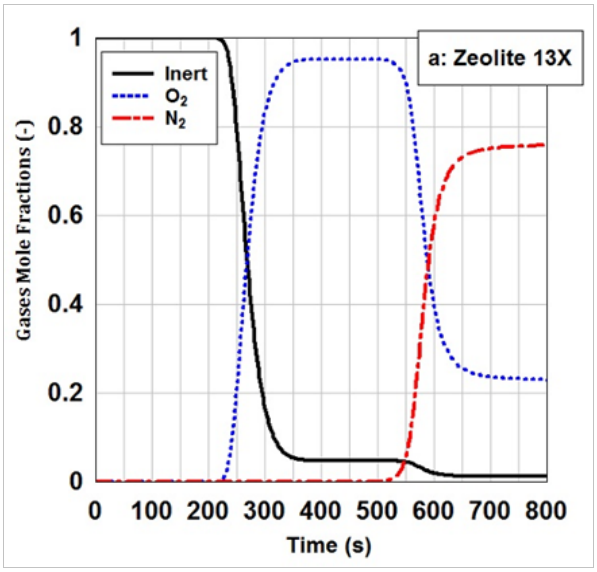

Figure 3 The simulated breakthrough curves of zeolite 13X for oxygen and nitrogen at adsorption pressure of 6 bar and feed flow rate of 5 LSTP/min. The adsorption bed was initially saturated with a non-adsorptive gas.

As time is passing, High Roll-up Phenomena is observed in the case of oxygen. Owing to High Roll-up Phenomena effect, oxygen concentration is approximately 4.5 times more than feed concentration during the time of 400-500seconds. Occurring High Roll-up Phenomena in the case of oxygen is due to this fact that there is a competitive adsorption between oxygen and nitrogen molecules to be adsorbed on the adsorbent. Oxygen is affected by the High Roll-up Phenomena because nitrogen adsorption on the adsorbent sites is much more than oxygen adsorption. Therefore, oxygen concentration is relatively increased rather than feed concentration. While time reaches nitrogen breakthrough at the time of 550seconds, oxygen concentration is starting to be reduced. As clearly shown in Figure 3, the High Roll-up Phenomena do not occur in the case of nitrogen due to its strong adsorption on zeolite 13X adsorbent.

The adsorption capacity in the adsorption bed depends on the factors such as pressure, temperature, flow rate.[2,12] Actually, the adsorption and desorption cycle of a PSA system operates by pressure increasing and decreasing. Adsorption and desorption phenomenon are inherently exothermic and endothermic, respectively. Therefore, optimal setting of temperature is very important owing to better performance of adsorption and desorption phenomenon. On the other hand, the adsorption of impurities on the adsorbent bed is a function of retention time on the adsorbent. Consequently, the flow rate factor is necessary for better performance of system. The concentration of nitrogen on zeolite 13X in terms of different adsorption pressures and time is presented in Figure 4. As pressure increases, the adsorption rate of more strongly adsorbed component increases.[2,12] As it is expected, nitrogen adsorption capacity on zeolite 13X enhances with pressure increasing. Oxygen concentrations along the bed length for zeolite 13X in different times have been depicted in Figure 5. Obviously, the slope of oxygen concentration curves is fast. The small MTZ for zeolite 13X has large adsorption rate. In the dynamic study of adsorption beds it is considerable to investigate desorption curves. The desorption curve of zeolite 13X is illustrated in Figure 6. In order to simulate desorption over the beds, it is assumed that a pure inert gas is utilized for cleaning the beds. By passing the inert gas through the bed in a pressure of 0.1bars, nitrogen with high concentration is first desorbed from top of the bed. As nitrogen is desorbed, a little adsorbed oxygen is removed from the bed with nitrogen. As time passes and the desorbed volume of nitrogen and oxygen gases decreases, the concentration of inert gas in the outlet of bed begins to increase.[22–27]

By referring to Figure 6:

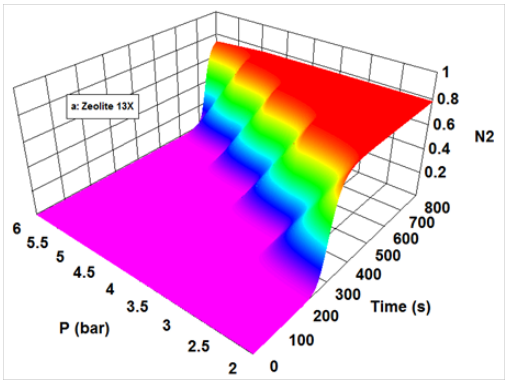

Figure 4 The outlet mole fraction of nitrogen form zeolite 13X at different adsorption pressures and feed flow rate of 4LSTP/min. The adsorption bed was initially saturated with a non-adsorptive gas.

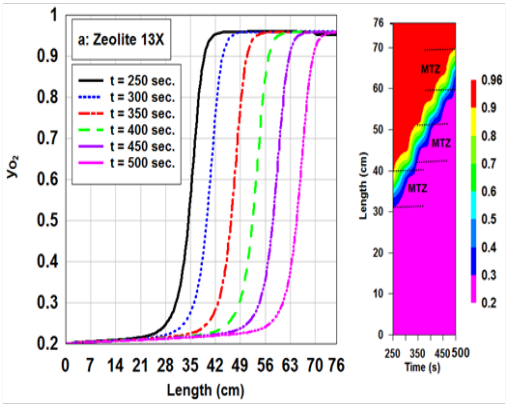

Figure 5 Distribution of oxygen concentration along the length of zeolite 13X during adsorption process in different times. The feed flow rate is 5LSTP/min and the adsorption pressure is 6bar.

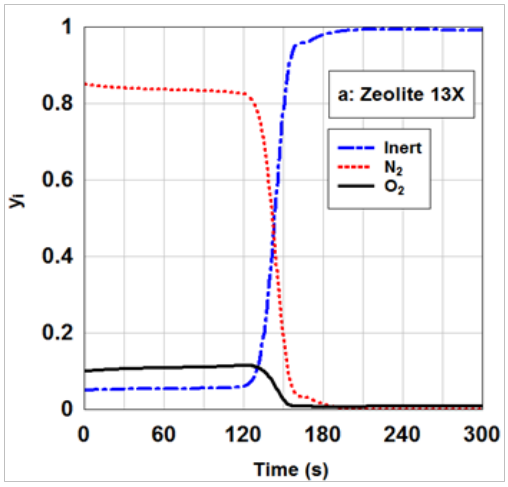

Figure 6 The outlet simulated concentration of gas phase from zeolite 13X during desorption at pressure of 0.1bar. The desorption bed was completely clean in the initial state.

Citation: Kakavandi IA, Shokroo EJ, Baghbani M, et al. Dynamic modeling of nitrogen adsorption on zeolite 13x bed. *Fluid Mech Res Int.* 2017;1(1):20–24. DOI: 10.15406/fmrij.2017.01.00004

The main drop of nitrogen concentration in the outlet of zeolite 13X occurs at the time of about 125seconds;

Nitrogen concentration in the outlet of zeolite 13X approaches zero after about 180seconds

Conclusion

Nitrogen adsorption on zeolite 13X bed is simulated. Desorption and adsorption dynamics of zeolite 13X was investigated in order to study the behavior of this zeolite.

The results obtained from dynamic simulation of bed showed that:

The High Roll-up Phenomena occurs for oxygen than nitrogen. There is a large mass transfer zone (MTZ) for zeolite 13X. Therefore, the adsorption rate of zeolite 13X is high. The main drop of nitrogen concentration in the outlet of zeolite 13X occurs at the time of about 125seconds. Nitrogen concentration in the outlet of zeolite 13X approaches zero after about 180seconds.[28–31]

Acknowledgments

None.

Conflicts of interest

Author declares that there is no conflicts of interest.

References

1. RM Milton. US Patent No. 2,882,243. 1959.
2. Ruthven DM, Farooq S, Knaebel KS. *Pressure Swing Adsorption*. New York: VCH Publications. 1994. 352 p.
3. DM Ruthven. *Principle of Adsorption and Adsorption Processes*. USA: John Wiley & Sons. 1984. 453 p.
4. CT Chou, Wen Chun Huang. Simulation of a Four-Bed Pressure Swing Adsorption Process for Oxygen Enrichment. *Industrial & Engineering Chemistry Research*. 1994;33(5):1250–1258.
5. L Lin. Numerical Simulation of Pressure Swing Adsorption Process. *Dissertation Presented for the Degree of Bachelor of Science*. XIDIAN University, China; 1997. 122 p.
6. JA Ritter, Yujun Liu. Tapered Pressure Swing Adsorption Columns for Simultaneous Air Purification and Solvent Vapor Recovery. *Ind Eng Chem Res*. 1998;37(7):2783–2791.
7. KG Teague, TF Edgar. Predictive Dynamic Model of a Small Pressure Swing Adsorption. *Ind Eng Chem Res*. 1999;38(10):3761–3775.
8. AMM Mendes, CAV Costa, AE Rodrigues. Analysis of Nonisobaric Steps in Nonlinear Bicomponent Pressure Swing Adsorption Systems: Application to Air Separation. *Ind Eng Chem Res*. 2000;39(1):138–145.
9. AMM Mendes, CAV Costa, AE Rodrigues. Oxygen Separation from Air by PSA: Modeling and Experimental Results Part I: Isothermal Operation. *Separation and Purification Technology*. 2001;24(1):173–188.
10. SJ Wilson. The Effects of a Readily Adsorbed Trace Component (Water) in a Bulk Separation PSA Process: The Case of Oxygen VSA. *Ind Eng Chem Res*. 2001;40(12):2702–2713.
11. SU Rege, K Qian, Buzanowski MA. Air-Prepurifcation by Pressure Swing Adsorption Using Single/Layered Beds". *Chemical Engineering Science*. 2001;56(8):2745–2759.
12. JG Jee, JS Lee, CH Lee. Air Separation by Small-Scale Two-Bed Medical O_2 Pressure Swing Adsorption. *Ind Eng Chem Res*. 2001;40(16):3647–3658.
13. JG Jee, JS Lee, CH Lee. Comparison of the Adsorption Dynamics of Air on Zeolite 5A and Carbon Molecular Sieve Beds" *Korean Journal of Chemical Engineering*. 2004;21(6):1183–1192.
14. JG Jee, JHJ Park, SJ Haam, et al. Effects of Nonisobaric Steps and Isobaric Steps on O_2 Pressure Swing Adsorption for an Aerator. *Ind Eng Chem Res*. 2002;41(17):4383–4392.
15. STY Choong, WR Peterson, DM Scott. On the Numerical Simulation of Rapid Pressure Swing Adsorption for Air Separation. *Jurnal Teknologi*. 2003;38:65–86.
16. JC Santos, AF Portugal, FD Magalhães, et al. Simulation and Optimization of Small Oxygen Pressure Swing Adsorption Units. *Ind Eng Chem Res*. 2004;43(26):8328–8338.
17. SP Reynolds, AD Ebner, JA Ritter. Enriching PSA Cycle for the Production of Nitrogen from Air. *Ind Eng Chem Res*. 2006;45(9):3256–3264.
18. KP Kostroski, PC Wankat. High Recovery Cycles for Gas Separations by Pressure-Swing Adsorption. *Ind Eng Chem Res*. 2006;45(24):8117–8133.
19. SJ Lee, JH Jung, JH Moon, et al. Parametric Study of the Three-Bed Pressure-Vacuum Swing Adsorption Process for High Purity O_2 Generation from Ambient Air. *Ind Eng Chem Res*. 2007;46(11):3720–3728.
20. JG Jee, MK Park, HK Yoo, et al. Adsorption and Desorption Characteristics of Air on Zeolite 5a, 10x, and 13x Fixed Beds. *Separation Science and Technology*. 2002;37(15):3465–3490.
21. M Mofarahi, EJ Shokroo. Comparison of Two Pressure Swing Adsorption Processes for Air Separation Using Zeolite 5A And Zeolite 13X. *Petroleum & Coal*. 2013;55(3):216–225.
22. CA Grande. Advances in pressure swing adsorption for gas separation. *ISRN Chemical Engineering*. 2012. 13 p.
23. Rosen M, Mulloth L, Affleck D, et al. Development and testing of a temperature-swing adsorption compressor for carbon dioxide in closed-loop air revitalization systems. *SAE international*. 2005. 8 p.
24. A Mivechian, Majid Pakizeh. Hydrogen recovery from Tehran refinery off-gas using pressure swing adsorption, gas absorption and membrane separation technologies: Simulation and economic evaluation. *Korean Journal of Chemical Engineering*. 2013;30(4):937–948.
25. SC Jang, S Yang, Seong Geun Oh. Adsorption dynamics and effects of carbon to zeolite ratio of layered beds for multi component gas adsorption. *Korean Journal of Chemical Engineering*. 2011;28(2):583–590.
26. YH Kim, DG Lee, DK Moon, et al. Effect of bed void volume on pressure vacuum swing adsorption for air separation. *Korean Journal of Chemical Engineering*. 2014;31(1):132–141.
27. M Zaman, JH Lee. Carbon capture from stationary power generation sources: A review of the current status of the technologies. *Korean Journal of Chemical Engineering*. 2013;30(8):1497–1526.
28. V Hoshyargar, F Fadaei, SN Ashrafizadeh. Mass transfer simulation of nanofiltration membranes for electrolyte solutions through generalized Maxwell-Stefan approach. *Korean Journal of Chemical Engineering*. 2015;32(7):1388–1404.
29. RT Yang. *Adsorbents: Fundamentals and Applications*. US: John Wiley & Sons; 2003. 425 p.
30. Olney TN, Cann NM, Cooper G, et al. Absolute scale determination for photoabsorption spectra and the calculation of molecular properties using dipole sum-rules. *Chemical Physics*. 1997;223:59–98.
31. S Jain, AS Moharir, P Li, et al. Heuristic design of pressure swing adsorption: a preliminary Study. *Separation and Purification Technology*. 2003;33(1):25–43.